Article details

Wang G., Zhai Y., Zhang S., Diomede L., Bigini P., Romeo M., Cambier S., Contal S., Nguyen N.H.A., Rosická P., Nickel C., Vijver M.G. & Peijnenburg W.J.G.M. (2020), An across-species comparison of the sensitivity of different organisms to Pb-based perovskites used in solar cells, Science of the Total Environment 708.
Doi: 10.1016/j.scitotenv.2019.135134

Science of the Total Environment 708 (2020) 135134

Contents lists available at ScienceDirect

Science of the Total Environment

journal homepage: www.elsevier.com/locate/scitotenv

An across-species comparison of the sensitivity of different organisms to Pb-based perovskites used in solar cells

Guiyin Wang [a,b], Yujia Zhai [b,h,*], Shirong Zhang [a,*], Luisa Diomede [d], Paolo Bigini [d], Margherita Romeo [d], Sebastien Cambier [e], Servane Contal [e], Nhung H.A. Nguyen [f], Petra Rosická [f], Alena Ševců [f], Carmen Nickel [g], Martina G. Vijver [b], Willie J.G.M. Peijnenburg [b,c]

[a] College of Environmental Science, Sichuan Agricultural University, Chengdu 611130, China
[b] Institute of Environmental Sciences (CML), Leiden University, P.O. Box 9518, 2300 RA, Leiden, the Netherlands
[c] National Institute of Public Health and the Environment (RIVM), P.O. Box 1, Bilthoven, the Netherlands
[d] Department of Molecular Biochemistry and Pharmacology, Istituto di Ricerche Farmacologiche Mario Negri IRCCS, 20156 Milan, Italy
[e] Environmental Research and Innovation (ERIN) Department, Luxembourg Institute of Science and Technology, 4422 Belvaux, Luxembourg
[f] Institute for Nanomaterials, Advanced Technologies and Innovation, Technical University of Liberec (TUL), Studentská 2, 46117 Liberec, Czech Republic
[g] Air Quality & Sustainable Nanotechnology, Institute of Energy and Environmental Technology (IUTA) e.V, 47229 Duisburg, Germany
[h] Oasen Water Company, P.O. Box 122, 2800AC, Gouda, The Netherlands

HIGHLIGHTS

- Multispecies toxicity assays were performed on Pb-based PSCs.
- Different dose–response was observed depending on the species.
- *V. fischeri* is the most sensitive model for detecting the toxicity of Pb-based PSCs.
- The results provide clue for the environmental risk assessment of Pb-based PSCs.

GRAPHICAL ABSTRACT

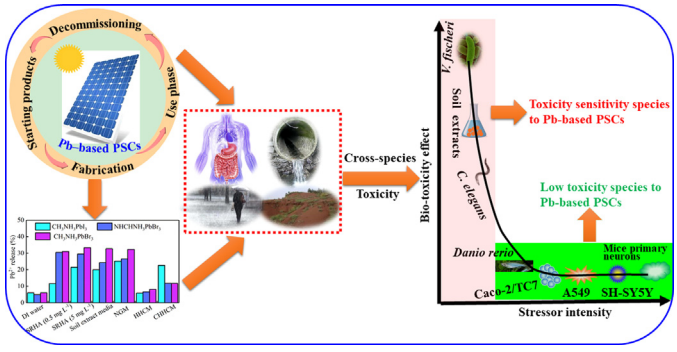

ARTICLE INFO

Article history:
Received 10 June 2019
Received in revised form 22 August 2019
Accepted 21 October 2019
Available online 21 November 2019

Editor: Julian Blasco

Keywords:
Perovskite solar cells
Lead
Toxicity
Dose response
3Rs

ABSTRACT

Organic–inorganic perovskite solar cells (PSCs) are promising candidates as photovoltaic cells. Recently, they have attracted significant attention due to certified power conversion efficiencies exceeding 23%, low–cost engineering, and superior electrical/optical characteristics. These PSCs extensively utilize a perovskite–structured composite with a hybrid of Pb-based nanomaterials. Operation of them may cause the release of Pb-based nanoparticles. However, limited information is available regarding the potential toxicity of Pb-based PSCs on various organisms. This study conducted a battery of *in vitro* and *in vivo* toxicity bioassays for three quintessential Pb-based PSCs ($CH_3NH_3PbI_3$, $NHCHNH_3PbBr_3$, and $CH_3NH_3PbBr_3$) using progressively more complex forms of life. For all species tested, the three different perovskites had comparable toxicities. The viability of Caco–2/TC7 cells was lower than that of A549 cells in response to Pb-based PSC exposure. Concentration–dependent toxicity was observed for the bioluminescent bacterium *Vibrio fischeri*, for soil bacterial communities, and for the nematode *Caenorhabditis elegans*. Neither of the tested Pb-based PSCs particles had apparent toxicity to *Pseudomonas putida*. Among all tested organisms, *V. fischeri* showed the highest sensitivity with EC_{50} values (30 min of exposure) ranging from 1.45 to 2.91 mg L^{-1}. Therefore, this study recommends that *V. fischeri* should be preferably utilized to assess.

* Corresponding authors.
E-mail addresses: y.zhai@cml.leidenunv.nl (Y. Zhai), srzhang01@aliyun.com (S. Zhang).

https://doi.org/10.1016/j.scitotenv.2019.135134

PSC toxicity due to its increased sensitivity, low costs, and relatively high throughput in a 96–well format, compared with the other tested organisms. These results highlight that the developed assay can easily predict the toxic potency of PSCs. Consequently, this approach has the potential to promote the implementation of the 3Rs (Replacement, Reduction, and Refinement) principle in toxicology and decrease the dependence on animal testing when determining the safety of novel PSCs.

1. Introduction

The ever–increasing global energy demand has accelerated the consumption of fossil fuel. Within the framework of the Paris agreement on climate change (Oztig, 2017), a quest for the reduction of fossil fuel consumption has been initiated, directed toward the utilization of green and renewable energy resources (Billen et al., 2019; Hauck et al., 2017; Maniarasu et al., 2018). Photovoltaic (PV) technology has generated considerable interest toward the quest for alternative green energy sources as it has the potential to relieve the reliance on fossil fuel and reduce the associated greenhouse gas emissions (Alaaeddin et al., 2019; Celik et al., 2018). One of the most promising alternatives is the use of solar cells with embedded perovskite structures. This application attracts growing interest because of their low–cost fabrication and superior photophysical properties (Billen et al., 2019; Jeon et al., 2018; Kayesh et al., 2018; Maniarasu et al., 2018; Zhou et al., 2019). These perovskite solar cells (PSCs) contain an organic–inorganic halide with an ABX_3 structure (Fig. S1A), where *A* represents an organic cation of methylammonium, formamidinium, and/or Cs^+, *B* represents a divalent metal such as Pb^{2+}, Sn^{2+}, or Ge^{2+}, and *X* represents a halogen such as Cl^-, Br^-, and/or I^- (Frost et al., 2014; Klug et al., 2017). Among them, Pb-based PSCs ($APbX_3$) have been shown to achieve power conversion efficiencies (PCEs) from an initial value of 3.8% to a certified value of 23.3% (Fig. S1B) (Billen et al., 2019; Jeon et al., 2018; Kayesh et al., 2018). However, their large–scale application requires that the solar cell design accounts for a reduction of potentially adverse environmental and human health effects, while sustainability requirements also need to be met. Therefore, it is essential to obtain a profound quantitative understanding of the fate and toxicity of Pb-based core materials of PSCs that are likely to exert adverse environmental effects.

With respecting to sustainability, several researchers have made seminal attempts to comprehend the potential environmental impacts of Pb-based PSCs focusing on their fabrication, use, and disposal. Recent studies combined with life cycle assessment stated that the environmental benefits of averting fossil fuel or grid electricity surpassed the environmental burden caused by the use of Pb-based PSCs, considering the emissions of potentially toxic substances (Billen et al., 2019; Celik et al., 2018; Hauck et al., 2017). Moreover, it has been demonstrated that potentially all Pb^{2+} from Pb-based PSCs might leak in response to rainfall once PSCs become permeable because of damage (Hailegnaw et al., 2015). However, when considering the amount of energy generated, the Pb emissions from Pb-based PSCs (as derived from rinsing during use) are still considerably lower than Pb emissions of a coal power plant (Hauck et al., 2017).

The toxicity of Pb^{2+} may be the key obstacle that restricts the broad commercial application of Pb-based PSCs (Maniarasu et al., 2018; Zhou et al., 2019). At their end–of–life stage, Pb-based PSCs are open structures, which easily dissociate and released Pb^{2+} into the environment in the presence of polar solvents such as water (Hailegnaw et al., 2015). Pb^{2+} is a very toxic contaminant. Efforts such as the homovalent substitution of Pb^{2+} with environmentally friendly cations (Sn^{2+}, Cu^{2+}, Ge^{2+}) have been devoted to improving the environmental safety of PSCs (Chen et al., 2019; Klug et al., 2017; Zhou et al., 2019). However, several Pb–free perovskites are still toxic, e.g., Sn–based PSCs have a higher or similar toxicity to zebrafish embryos than Pb-based PSCs because of their strong acidification (Babayigit et al., 2016; Bae et al., 2019). In addition, completely substituting Pb^{2+} with the above–mentioned candidates still poses an enormous challenge because of the limited of PCEs of alternatives and/or their poor suitability for PV applications as a result of high instability of their divalent state by fast oxidation kinetics (Kayesh et al., 2018; Tavakoli et al., 2018).

Proper understanding of the toxicity of Pb-based PSCs is essential since these PSCs are used for large–scale commercialization and help to shape the future PV cell development toward 'green/safe(r)–by–design' ambitions. To collect toxicity data, modelling or toxicity tests are preferably performed following a 3Rs (Replacement, Reduction, and Refinement) strategy, which advocates the reduction or replacement of vertebrates (Campana and Wlodkowic, 2018; Hristozov et al., 2016). Considering the current international trend of adhering to 3Rs principles, convenient, rapid, and cost–effective *in vitro* toxicity assays derived from non–vertebrate models and cell lines are often required. These maintain a high degree of scientific reliability and provide reasonable feedback on their efficiencies (Barrick et al., 2019). Recently data were published on the impacts of $CH_3NH_3PbI_3$ on various cellular models such as murine primary hippocampal neurons, human dopaminergic neuroblastoma cells, and human lung adenocarcinoma epithelial cells (Benmessaoud et al., 2016). Other studies reported the *in vivo* toxicity data of various PSCs for *Daphnia magna* and zebrafish (Babayigit et al., 2016; Zhou et al., 2018). Those groundbreaking efforts extended our horizons toward recognizing the potential risks of Pb^{2+} leakage from Pb-based PSCs into non–vertebrate organisms and the human body. However, little systematic information is available on the comprehensive environmental toxicity of Pb-based PSCs from the perspective of non–vertebrate organisms to fulfill the principles of the 3Rs.

The present study, therefore, employed three representative Pb-based PSCs with different *A*–site or *X*–site elements and evaluated their dissolution and aggregation. The main aims of this study were to (i) systematically generate toxicity data for Pb-based PSCs using a suite of environmental models from single aquatic and soil bacterial species, to *Caenorhabditis elegans* as a representative invertebrate animal model living in the soil, and to progressively more complex forms of life such as human cell lines; (ii) identify the most sensitive bioassay. The presented results provide more information on the ecological impacts of Pb-based PSCs, which is vital for their large–scale fabrication and commercialization, and for the future development of PV cells that are safe by design.

2. Materials and methods

2.1. Preparation and characterization of perovskites

The three Pb-based PSCs $CH_3NH_3PbI_3$, $NHCHNH_3PbBr_3$, and $CH_3NH_3PbBr_3$ were obtained from the Ecole Polytechnique Federale de Lausanne (Lausanne, Switzerland). Their stock suspensions ($10\ g\ L^{-1}$) were prepared by adding perovskite powders to sterilized deionized water, which was followed by 16 min of ultrasonication

(400 W) to break the developed aggregates and enhance their stability prior to the experiments. The suspensions were prepared by applying the Standard Operation Procedure (SOP) developed under the generic NANOGENOTOX dispersion protocol (Jensen et al., 2011). All suspensions were freshly prepared immediately before the experiments.

The morphology of these Pb-based PSCs was observed by scanning electron microscopy (SEM, Vega3, Tescan Co. Ltd., Brno, Czech Republic). The size distribution and zeta potential of Pb-based PSCs mixed with natural organic matter (NOM, 0.5 and 5.0 mg L^{-1}) and Ca^{2+} (5 and 10 mmol L^{-1}) were measured by dynamic light scattering (DLS) spectroscopy in a Zetasizer Nano ZS instrument (Malvern Instruments, Malvern, UK). Details were available in Section S1 of the SI.

2.2. Solubility experiments

The release of soluble Pb^{2+} from Pb-based PSCs was quantified in different exposure media at a concentration of 100 mg L^{-1}. The following exposure media were used: deionized water, deionized water supplemented with Suwannee River humic acid (SRHA), a soil extract, nematode growth medium (NGM), high–hardness combo media (HHCM), and a conditioned high–hardness combo medium (CHHCM). Table S1 provides the composition of the exposure media. The exposure media were shaken for 24 h after addition of the Pb-based PSCs. Then, the suspensions were centrifuged for 30 min at 4 °C and filtered through a 0.02 μm syringe filter (Anotop10, Whatman, USA). Part of the filtrate was surveyed by SEM to detect remaining particles; however, no such particles were found, suggesting that the filtration was effective. Subsequently, the filtrates were acidified with HNO_3 and diluted to a detectable concentration. Pb^{2+} in the supernatant was analyzed by inductively coupled plasma optical emission spectrometry (ICP–OES, Optima 5300 DV, PerkinElmer, Waltham, MA, USA).

2.3. Toxicity tests

Several bioassays were conducted to estimate the toxicity of Pb-based PSCs and to identify the sensitivity of different organisms to them in the environment. Toxicity tests were conducted using six species, including a marine photobacterium (*Vibrio fischeri*), a soil microorganism (*Pseudomonas putida*), natural microbes extracted from soil, a nematode *Caenorhabditis elegans*, and human cell models (human lung adenocarcinoma cell line, A549 and human colonic epithelial CaCo–2 subclone TC7 cells, Caco–2/TC7). Respecting species–specific features and sensitivity, different exposure concentrations were used, based on previously performed pilot tests. The reason for preparing different tested concentrations of Pb-based PSCs is based on the released amount of Pb^{2+} from PSCs and the different toxicity of Pb^{2+} to various organisms. Toxicity test procedures were performed following ISO protocols (ISO, 1999, 2007, 2010) and previously published studies (Baderna et al., 2014; Esquivel-Gaon et al., 2018; Zhai et al., 2017).

2.3.1. Vibrio fischeri bioluminescence inhibition assay

The toxicity test for the photobacterium *V. fischeri* (strain NRRL–B–11177, DSMZ, Germany) was performed using the Microtox® Synergy 2 analyser (Biotek Instruments, Inc, Winooski, VT, USA) following the ISO 11348–3 guidelines in a 96–well plate format (ISO, 2007). Dehydrated *V. fischeri* (a seawater Gram–negative model bacterium) were activated by a reconstitution solution (ultrapure water) immediately before the test. Both control and samples were adjusted to an osmotic pressure of approximately 2% salinity with an osmotic adjustment solution containing 22% NaCl. After preliminary tests, nine concentrations of each Pb-based PSCs (ranging from 0 to 66.7 mg L^{-1}) were prepared and sonicated. After 30 min of incubation with the Pb-based PSCs under constant temperature (15 °C) in microplates, the bacterial luminescence intensities were recorded with an excitation source at 490 nm wavelength. For each treatment and control, three biological replicates were conducted. The inhibitory effects were evaluated by taking the ratio of the decrease in bacterial light production to the remaining light.

2.3.2. Pseudomonas putida toxicity assay

The toxicity of Pb-based PSCs for *P. putida* was assessed with a modified version of ISO 9408 (ISO, 1999) and previously described protocols in Esquivel-Gaon et al., (2018) for the evaluation of the hazard of nanomaterials. The pre–culture method of bacteria was demonstrated in the Section S2 of the SI. Bacterial growth upon exposure to Pb-based PSCs suspensions (0–100 mg L^{-1}) was induced at 27 °C for 24 h in a 96–well plate. Samples of *P. putida* cells in bacterial culture without PSCs suspension and with Pb $(NO_3)_2$ (0–1000 mg L^{-1}) were run as a negative control and reference control, respectively. The growth rate was measured based on the optical density of samples at 600 nm (OD_{600}), measured every 2 h over a total of 6 h by a Synergy HTX plate reader (Biotek Instruments, Inc, Winooski, VT, USA). The bacterial growth rate was defined by linear regression of absorbance unit (AU) of the sample versus exposure time (h). The cell viability of *P. putida* cultures that were exposed to Pb-based PSCs (0–500 mg L^{-1}) was detected using the LIVE/DEAD BacLight viability kit (L7012, Molecular Probes, Inc., Eugene, OR) following the protocol developed by Jalvo et al. (2017). Briefly, each sample (1 mL) was transferred to a 96–well plate and incubated at 27 °C for 6 h and 24 h. Subsequently, bacteria (100 μL) were moved to another plate, staining fluid (100 μL) was added, and the samples were incubated in dark for 15 min. After this incubation, the proportion of live (excitation/emission, 485/528 nm) and dead cells (excitation/emission, 485/645 nm) was determined using the Synergy HTX plate reader. For positive ion control, the same concentration of $Pb(NO_3)_2$ was tested. All growth rate and cell viability experiments were conducted in triplicates. Additionally, the respiration activity of nitrifying microorganisms in the activated sludge was monitored over 24 h at 27 °C when exposed to all three types of Pb-based PSCs suspensions. Pb^{2+} at the same concentrations that were determined for each PSC material (as presented in Fig. S2) acted as positive reference control. The detailed procedures were listed in SI under Section S3. The oxygen consumption rate (mg O_2 $L^{-1}h^{-1}$) and cumulative oxygen consumption (mg O_2 L^{-1}) were continuously monitored using a twelve–channel Micro–Oxymax® respirometer (Columbus Instruments, Columbus, USA). Respiratory experiments were carried out in duplicate.

2.3.3. Assay of soil bacterial community extracts

The ability of soil microbial communities to utilize numerous carbon sources after Pb-based PSC exposure was determined with a community–level substrate utilization test via direct incubation of soil extracts in a Biolog EcoPlate (Biolog Inc., Hayward, USA) containing 31 different carbon sources (Table S2). Fresh soil samples and soil suspensions were prepared as previously described (Zhai et al., 2017). Diluted soil extracts (100 μL) containing Pb-based PSCs (2.45–37.52 mg L^{-1}) were added to the wells of a Biolog plate until a final volume of 150 μL was reached and the mixture was incubated in dark at 25 °C for 96 h under sterile conditions. The optical density (at a wavelength of 590 nm) of each well was measured every 24 h using an ELx808 ELISA microplate reader (BioTek Instruments, Inc., Winooski, VT, USA) to ensure saturation of the utilized substrates. The average well color development (AWCD) of each microplate was calculated as previously described (Zhai et al., 2017) to assess the microbial activity. This technique identi-

fies microbial communities and identifies, which substrates are exploited the most by these communities (Pino-Otín et al., 2019). This technique was recently developed to be suitable to analyze the effects of toxicants (Deary et al., 2018). The influence of $PbCl_2$ (1.49–24.39 mg L^{-1}) was assayed as a positive reference to evaluate the toxicity of Pb^{2+}. The negative control treatment comprised a soil extract that was dosed with buffer instead of Pb-based PSCs. For each group, triplicate microcosms were assessed per Ecoplate.

2.3.4. Caenorhabditis elegans assay

The toxicity of Pb-based PSCs for *C. elegans* was measured according to standard methods (Baderna et al., 2014; ISO, 2010). The information regarding worm strains and culture was included in SI, Section S4. In the bioassay, nematodes were synchronized at the L3–L4 larval stages, were collected with M9 buffer, centrifuged, and washed twice with 5 mmol L^{-1} phosphate buffered saline (pH 7.4), to eliminate bacteria. The nematodes (100 worms/100 μL) were incubated with Pb-based PSCs (0–20 mg L^{-1}) without *Escherichia coli* OP50, to avoid any potential interference. Control nematodes (100 worms/100 μL) were incubated with water. After 2 h of incubation on an orbital shaking plateau in dark at 20 °C, nematodes were spotted on one side of the nematode growth medium agar plate in the absence of bacteria. On the other side of the plate, *E. coli* was spotted as food. The number of worms that moved to the food after 24 h were identified as being alive. Four replicates were conducted to evaluate the survival of soil nematodes.

2.3.5. Cytotoxicity measurements

A549 cells were purchased from the American Type Culture Collection (Manassas, VA, USA), while the Caco–2/TC7 cells were a generous gift from Dr. Monique Rousset (Institute National de la Santé et de la Recherche Médicale, INSERM, France). The cell culture procedures were presented in SI, Section S5. For the toxicity assay, cells were first incubated for 24 h at 37 °C in 96–well plates, at 1.2 × 10^5 cells mL^{-1}, in 150 μL of Dulbecco's Modified Eagle Medium (Georgantzopoulou et al., 2016; Klein et al., 2017; Esquivel-Gaon et al., 2018). Subsequently, cells were treated with different concentrations of Pb-based PSCs (0–100 mg L^{-1}) and incubated for at least 24 h in a CO_2–incubator. Three pre–incubated modes were tested, including the addition of Human serum (HS), Bovine serum (BS), and no serum (NS) addtion. Thereafter, the media in each well was discarded and MTT solution (3–(4,5–dimethylthiazol–2–yl)–5–(3–carboxymethoxy–phenyl)–2–(4–sulfophenyl)–2H–tetrazolium, Promega) was added to each well. The cell viability was measured using a Synergy 2 plate reader at 490 nm after 1 h in an incubator at 37 °C in dark. At least three independent experiments were performed with a minimum of three replicates of each Pb-based PSCs concentration in each plate.

2.4. Statistical analyses

Data from all experiments were analyzed by one–way analysis of variance (ANOVA), which was followed by a Tukey's multiple comparison test using SPSS software (version 24.0; SPSS, Inc., Chicago, IL, USA) and the results were expressed as means with standard deviations. Throughout, a significance level of $P < 0.05$ was applied. The toxicity of Pb-based PSCs on the different tested species was reported as EC_{50} values (50% effective concentration) with 95% confidence intervals. Monophasic concentration–response curves for endpoints of organisms were fitted with GraphPad Prism 8.0 (GraphPad Software, San Diego, CA, USA) by non–linear regression analysis using a four–parameter Hill model. All figures were plotted using OriginPro 9.0 (OriginLab Corporation, Northampton, MA, USA).

3. Results

3.1. Characterization of Pb-based perovskite solar cells

The Pb-based PSCs $CH_3NH_3PbI_3$, $NHCHNH_3PbBr_3$, and $CH_3NH_3PbBr_3$ had cuboidal and hexagonal morphologies with smooth surfaces (Fig. 1). Although the size of $CH_3NH_3PbI_3$ reached the micron range at ~50 μm, this was not the case for $NHCHNH_3PbBr_3$ and $CH_3NH_3PbBr_3$ and the aggregates of the latter two can be clearly observed in Fig. 1B and C via agglomerates with irregular shapes. The hydrodynamic diameters and zeta–potentials (Table S3) of Pb-based PSCs suspensions mixed with different types of NOM and Ca^{2+} were measured by DLS. A change in the size of Pb-based PSCs aggregates was not noticeable upon addition of NOM and Ca^{2+}, except for the combination of 5 mg L^{-1} Suwannee river fulvic acid and 0.005 mol L^{-1} Ca^{2+}. The zeta potential values indicated that the surface of the Pb-based PSCs particles is negatively charged (−13.00–−2.50 mV for $CH_3NH_3PbI_3$, −15.48–−4.28 mV for $CH_3NH_3PbBr_3$, and −14.35–−3.97 mV for $NHCHNH_3PbBr_3$, respectively). No marked change was found in the zeta potential among the three types of Pb-based PSCs.

A difference in the solubility of Pb-based PSCs particles was evident in different exposure medium (Fig. S3). All three Pb-based PSCs (100 mg L^{-1}) were slightly soluble (<12.0%) under the tested conditions in deionized water, HHCM, and CHHCM culture media after 24 h of incubation except for $CH_3NH_3PbI_3$ in the CHHCM culture medium (22.6%). However, their solubility in the remaining exposure media was relatively high since up to 33.5% of the Pb-based PSCs particles were dissolved after 24 h. The percentage of Pb^{2+} release increased with increasing SRHA concentrations. Overall, there was a higher Pb^{2+} release of $CH_3NH_3PbBr_3$ compared with $CH_3NH_3PbI_3$ and $NHCHNH_3PbBr_3$ in the tested media.

3.2. Toxicity evaluation of Pb-based perovskite solar cells on Vibrio fischeri

The inhibitory effects of tested Pb-based PSCs on the bioluminescence intensity of *V. fischeri* increased with increasing PSC concentrations, following a dose–response relationship. Although this relationship was analogous, the bioluminescence inhibition of *V. fischeri* increased remarkably with increasing $CH_3NH_3PbI_3$ concentrations from 0.52 to 66.7 mg L^{-1} (Fig. 2A, $P < 0.05$), while $NHCHNH_3PbBr_3$ concentrations ranged from 0.52 to 33.3 mg L^{-1} (Fig. 2B, $P < 0.05$) and $CH_3NH_3PbBr_3$ concentrations from 0.52 to 16.7 mg L^{-1} (Fig. 2C, $P < 0.05$). The inhibition rates reached 99.31, 91.46, and 94.18% compared to the control treatment at maximum tested concentration (66.7 mg L^{-1}) for $CH_3NH_3PbI_3$, $NHCHNH_3PbBr_3$, and $CH_3NH_3PbBr_3$, respectively. Specifically, the corresponding EC_{50} values (30 min) for *V. fischeri* were 2.18 (1.17–3.63), 1.45 (1.11–1.82), and 2.91 (2.25–3.72) mg L^{-1}, respectively (Table 1). This indicates lower toxicity of $CH_3NH_3PbBr_3$ compared with the other two PSCs, although the confidence intervals largely overlap.

3.3. Effect of Pb-based perovskite solar cell exposure on the growth rate, cell viability, and respiration activity of Pseudomonas putida

Recently, perovskite particles were reported to possess antibacterial ability (Shah et al., 2018). Here, Pb-based PSCs were exposed to a *P. putida* culture with the aim to determin their effects on bacterial growth (Fig. 3, 24 h of exposure) and cell viability (Figs. S4 and S5, 6 and 24 h of exposure, respectively). The obtained bacterial growth rates were clearly restrained after exposure to Pb^{2+} at concentrations above 200 mg L^{-1} (Fig. S6, $P < 0.05$). In contrast, a promotional effect on the growth rate of *P. putida* was observed after exposure to Pb-based PSCs at a concentration up to 100 mg

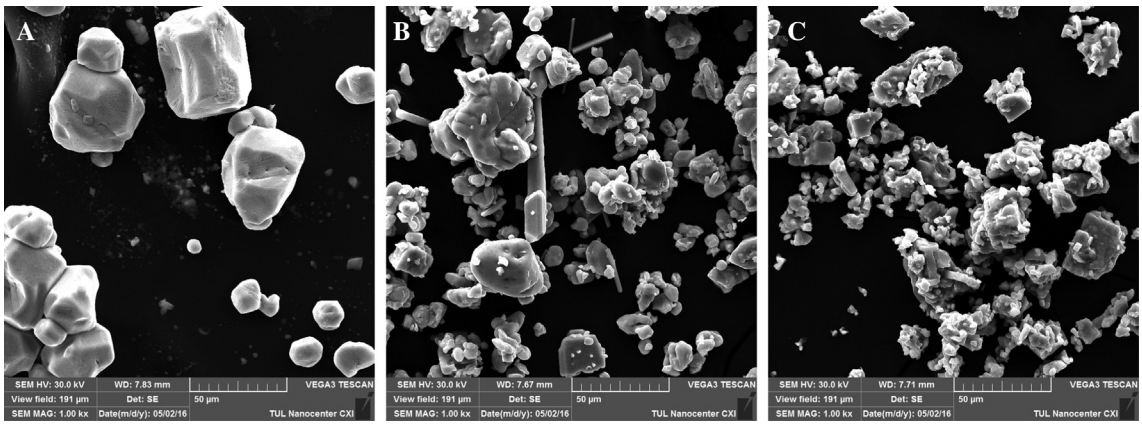

Fig. 1. SEM images of Pb-based PSCs (A, $CH_3NH_3PbI_3$; B, $NHCHNH_3PbBr_3$; C, $CH_3NH_3PbBr_3$) in sterilized deionized water (10 g L^{-1}).

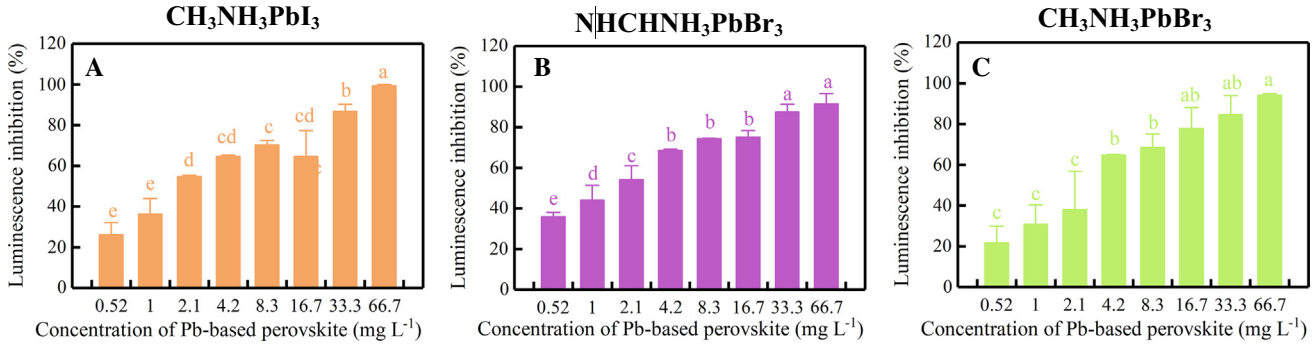

Fig. 2. Effects of Pb-based PSCs on the toxicity to *V. fischeri*. The same lowercase in the figure indicates that the results under different exposure concentrations of Pb-based PSCs are not significantly different according to the Tukey's test at $P < 0.05$. Error bars represent standard deviations.

L^{-1} (Fig. 3). Similarly, the particles also did not affect bacterial cell viability (Fig. S4). Concentration–response toxicity relationships were not found for both growth rate and cell viability in the exposure treatments. Thus, EC_{50} values could not be reliably established for these endpoints.

Moreover, the effect of Pb-based PSCs exposure on the respiration activity of *P. putida* was evaluated based on the quantification of the O_2 consumption rate and the accumulation of O_2 production (Fig. 4). Compared with the control treatment (Fig. 4D and H), the O_2 consumption rate and cumulative O_2 production of bacteria increased in response to Pb-based PSCs exposure, indicating that there was no direct adverse impact on the bacteria. The O_2 consumption rate reached a maximum value after 6–8 h of incubation, after which, it strongly decreased and stabilized after 20 h. However, different decreasing amplitudes of the O_2 consumption rate were observed among the three Pb-based PSCs. The decrease was rapid in the $CH_3NH_3PbBr_3$ exposure group, implying that the toxicity of $CH_3NH_3PbBr_3$ was higher than that of the other two PSCs. The changing trend of the cumulative O_2 production was similar to that of the O_2 consumption rate (Fig. 4E–H). The total accumulated amounts of produced O_2 in the presence of $CH_3NH_3PbI_3$ (2330–2764 mg L^{-1}), $NHCHNH_3PbBr_3$ (2098–2524 mg L^{-1}), and $CH_3NH_3PbBr_3$ (2116–2423 mg L^{-1}) clearly exceeded that of the control (1860–2162 mg L^{-1}) during the 24 h incubation. The Pb-based PSCs may promote the gas exchange across activated sludge, which increases the metabolic activity of bacteria involved in the ammonia oxidation.

3.4. Responses of bacterial communities to soil extracts following Pb-based perovskite solar cell exposure

Exposure of soil extracts to different concentrations of Pb-based PSCs resulted in a trend, which was analogous to the trend observed in case of exposure to Pb^{2+}; however, a slightly higher metabolic potential of bacterial communities (AWCD values) was found (Fig. 5). The metabolic potential decreased with increasing Pb-based PSC concentrations, and a pronounced effect was detected at concentrations exceeding 2.45 mg L^{-1}. The EC_{50} value derived from the Pb^{2+} curve was 5.47 (4.96–6.03) mg L^{-1}, which was significantly lower than that of any of the Pb-based PSCs (Table 1). This implies that Pb^{2+} toxicity to soil bacterial communities was higher than that of Pb-based PSCs. A comparison of the EC_{50} values of the Pb-based PSCs types (Table 1) confirmed that the $CH_3NH_3PbBr_3$ was the most noxious of the Pb-based PSCs to soil microbes with an EC_{50} value of 8.07 (6.65–9.85) mg L^{-1}, followed by $CH_3NH_3PbI_3$ with an EC_{50} value of 9.27 (7.96–10.76) mg L^{-1}, and $NHCHNH_3PbBr_3$ with an EC_{50} value of 12.81 (10.64–15.34) mg L^{-1}. The overlap of the confidence intervals indicates marginal differences in toxicity cross the tested PSCs.

3.5. Toxic effects of Pb-based perovskite solar cells on Caenorhabditis elegans

Surprisingly, only negligible toxic effects were found at concentrations up to 10 mg L^{-1} in the acute assay (Fig. 6). The exception was the group exposed to $CH_3NH_3PbI_3$, for which the survival of *C. elegans* (68.75%) was far lower than that of the control group (Fig. 6A, $P < 0.05$). The survival of *C. elegans* decreased to 6.70, 13.93, and 22.11% at a concentration of 10 mg L^{-1} for $CH_3NH_3PbI_3$, $NHCHNH_3PbBr_3$, and $CH_3NH_3PbBr_3$, respectively ($P < 0.05$).The corresponding EC_{50}–values for the survival of *C. elegans* indicated that $CH_3NH_3PbI_3$ (11.73 (11.49–11.98) mg L^{-1}) was consistently the most toxic PSC, followed by $NHCHNH_3PbBr_3$ (15.01 (14.18–16.00) mg L^{-1}) and $CH_3NH_3PbBr_3$ (15.38 (15.08–15.67) mg L^{-1}) (Table 1). No effects

Table 1
Effect levels as estimated for different species exposed to Pb-based PSCs.

Pb-based PSC	Test species	Duration	Effect	Test procedure	EC_{50} value (mg L^{-1})[a]
$CH_3NH_3PbI_3$	A549	24 h	Cell viability	Esquivel-Gaon et al., (2018)	>100
	Caco–2/TC7	24 h	Cell viability	Esquivel-Gaon et al., (2018)	99.97–229.70 (84.06–266.30)
	V. fischeri	0.5 h	Luminescence inhibition	ISO 11348–3 protocol (ISO, 2007)	2.18 (1.17–3.63)
	C. elegans	24 h	Survival	ISO 10,872 protocol (ISO, 2010)	11.73 (11.49–11.98)
	P. putida	6 h and 24 h	Mortality	ISO 10,712 protocol (ISO, 1995)	NC[c]
	Soil extracts	96 h	Growth inhibition	Zhai et al., (2017)	9.27(7.96–10.76)
	Danio rerio (Babayigit et al., 2016)	4 dpf[b]	Survival	OECD test guidelines No. 236 (OECD, 2013)	106.03 g L^{-1}[d]
	SH–SY5Y(Benmessaoud et al., 2016)	72 h	Cell mortality	Benmessaoud et al., (2016)	>100
	Mice primary neurons (Benmessaoud et al., 2016)	72 h	Cell mortality	Benmessaoud et al., (2016)	>200
$CH_3NH_3PbBr_3$	A549	24 h	Cell viability	Esquivel-Gaon et al., (2018)	>100
	Caco–2/TC7	24 h	Cell viability	Esquivel-Gaon et al., (2018)	66.48–114.60(57.38–176.08)
	V. fischeri	0.5 h	Luminescence inhibition	ISO 11348–3 protocol (ISO, 2007)	2.91 (2.25–3.72)
	C. elegans	24 h	Survival	ISO 10,872 protocol (ISO, 2010)	15.38 (15.08–15.67)
	P. putida	6 h and 24 h	Mortality	ISO 10,712 protocol (ISO, 1995)	NC[c]
	Soil extracts	96 h	Growth inhibition	Zhai et al., (2017)	8.07 (6.65–9.85)
$NHCHNH_3PbBr_3$	A549	24 h	Cell viability	Esquivel-Gaon et al., (2018)	>100
	Caco–2/TC7	24 h	Cell viability	Esquivel-Gaon et al., (2018)	110.20–179.40 (56.27–233.08)
	V. fischeri	0.5 h	Luminescence inhibition	ISO 11348–3 protocol (ISO, 2007)	1.45 (1.11–1.82)
	C. elegans	24 h	Survival	ISO 10,872 protocol (ISO, 2010)	15.01(14.18–16.00)
	P. putida	6 h and 24 h	Mortality	ISO 10,712 protocol (ISO, 1995)	NC[c]
	Soil extracts	96 h	Growth inhibition	Zhai et al., (2017)	12.81(10.64–15.34)

[a] EC_{50}, 50% effective concentration; Values in parentheses are the 95% confidence intervals
[b] dfp, day post fertilization
[c] NC, not calculable because there was no relationship between the Pb-based PSCs concentrations in the exposure medium and the cell mortality of *P. putida* or growth rate
[d] Based on the nominal concentrations of PbI_2.

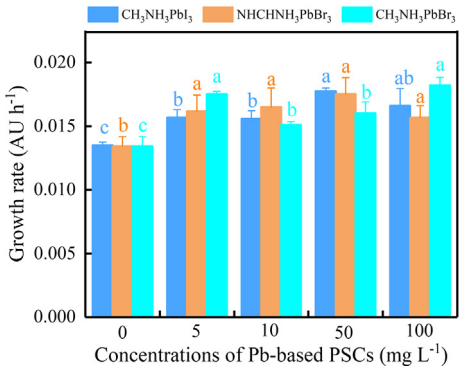

Fig. 3. Growth rate of *P. putida* exposed for 24 h to the Pb-based PSCs. The bars represent the median ± SD of three independent experiments, assayed in triplicate. The same lowercase letters above at bar indicate that the results obtained under different exposure concentrations of the same Pb-based PSCs are not significantly different according to the Tukey's test at $P < 0.05$.

on the survival of *C. elegans* (100%) were observed in the control group.

3.6. Cytotoxicity of Pb-based perovskite solar cells against human cancer cell lines

The Pb-based PSCs showed slight cytotoxic activity against A549 cells over the entire concentration range (Fig. 7A, 1–100 mg L^{-1}). In contrast, Caco–2/TC7 cells were sensitive to Pb-based PSCs and their viabilities decreased in a concentration–dependent manner. Pb-based PSCs considerably impeded the growth of Caco–2/TC7 cells, inhibiting 42.79–63.46% of cells compared with the control (Fig. 7B, $P < 0.05$) at an exposure dose of 100 mg L^{-1}. No obvious cytotoxicity changes were observed in the pre–incubated modes. $CH_3NH_3PbBr_3$ was the most toxic of the tested PSCs as it induced a remarkable decline in cell viability, especially at concentrations > 10 mg L^{-1} in both cell types. Information on the Pb-based PSCs–mediated cytotoxicity is limited and therefore, further experiment are indispensable to assess the toxicity mechanisms underlying the impacts of these promising PV materials on cells.

4. Discussion

4.1. Environmental behavior of Pb-based perovskite solar cells

The toxicity of nanoparticles (NPs) strongly depends on their physical–chemical characteristics, such as their chemical composition, size distribution, degree of agglomeration, surface coating, and dissolution potential (Bondarenko et al., 2016; Moon et al., 2019; Zhai et al., 2017). The size–dependent toxic effects of NPs toward bacteria (Nguyen et al., 2018; Ševců et al., 2017; Zhai et al., 2017), *C. elegans* (Moon et al., 2019), and A549 cells (Wang et al., 2018) that have previously been reported, generally indicated that particles of smaller sizes conveyed stronger toxicity. Recent data also showed that cubic–shaped carbon nanomaterials caused higher toxicity than tube–shaped graphitic nanomaterials to *D. magna* (Bacchetta et al., 2018). In addition, in *C. elegans*, rod–shaped titanium dioxide NPs induced stronger toxicity than bipyramidal particles. This indicates that the shape can strongly influence the toxicity of NPs (Iannarelli et al., 2016). Based on the

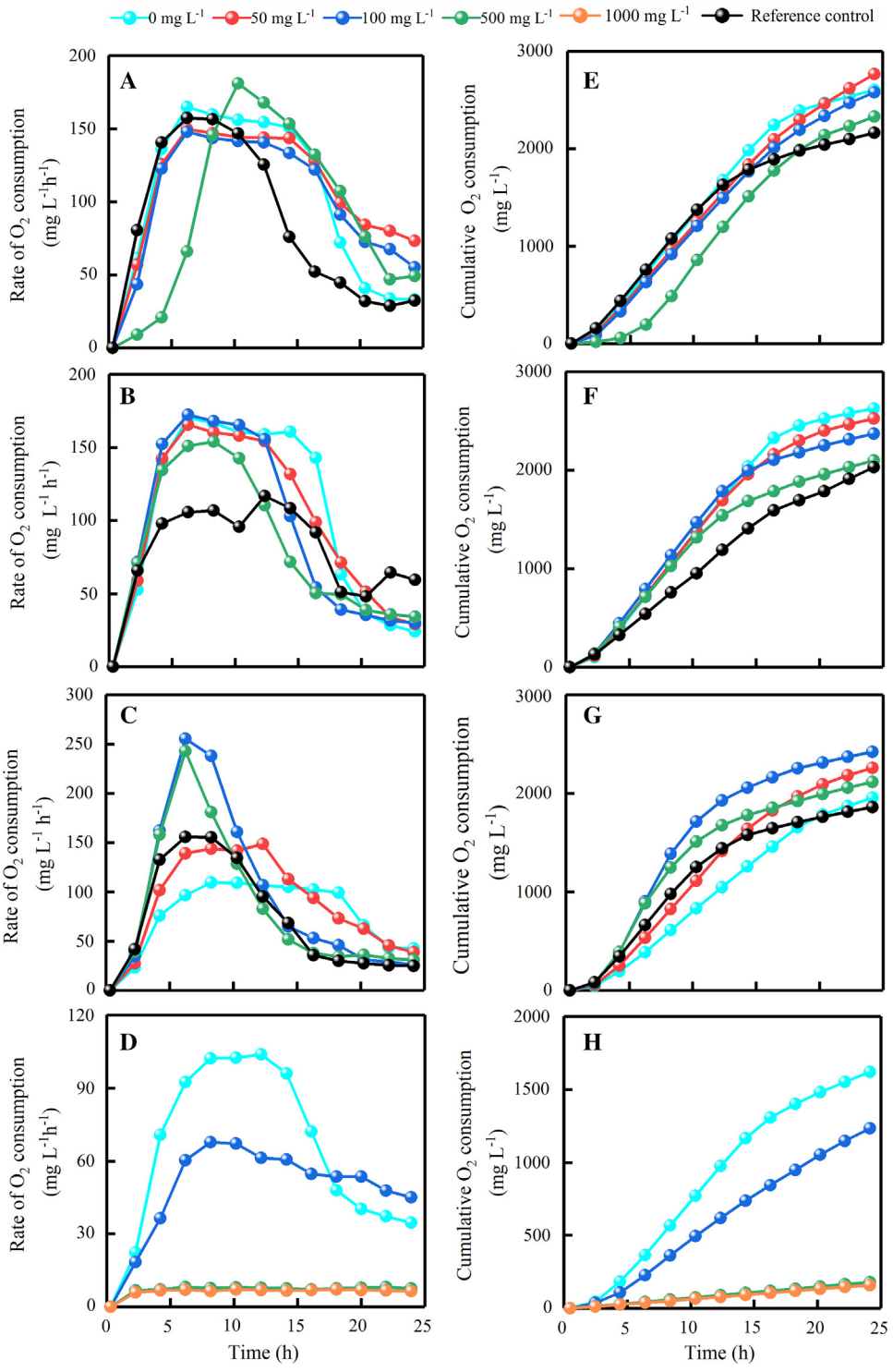

Fig. 4. Respiration activity of *P. putida* exposed to $CH_3NH_3PbI_3$ (A and E), $NHCHNH_3PbBr_3$ (B and F), $CH_3NH_3PbBr_3$ (C and G) Pb-based PSCs dispersions and Pb^{2+} (D and H) for 24 h. Left–side plots: O_2 consumption rate, and right-side plots: cumulative O_2 consumption. Each curve represents the media of three independent experiments, assayed in duplicate.

results of this study (Table 1), $NHCHNH_3PbBr_3$ and $CH_3NH_3PbBr_3$–triggered toxicities were generally higher than that of $CH_3NH_3PbI_3$. The toxicity of Pb-based PSCs may be caused (either mainly or partly) by Pb^{2+} released from the Pb-based core materials of PSCs. This was further corroborated by the Pb^{2+}–release profiles since the dissolution of $CH_3NH_3PbBr_3$ and $NHCHNH_3PbBr_3$ in different exposure media exceeded that of $CH_3NH_3PbI_3$ (Fig. S3). Indeed, numerous papers have previously identified the release of toxic ions from metal–containing NPs as the central factor that contributes to their ecotoxicity (Bondarenko et al., 2016; Ng et al., 2019). In the case of metal oxide NPs (e.g. ZnO, CuO) (Dankers et al., 2018; Wang et al., 2018), the formation of cations is the predominant determinant of toxicity because free ions are assumed to enter and accumulate in organisms more easily than larger particles. Although the toxic effects of metal ions dissolved in the exposure medium to environmentally relevant organisms are

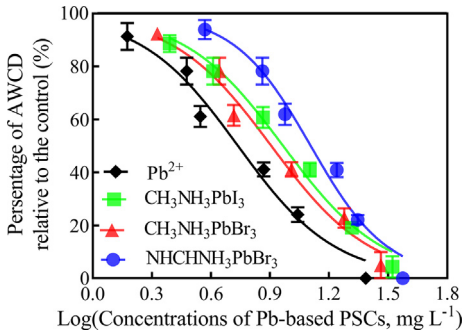

Fig. 5. Dose–response curves of AWCD of soil extracts exposed to different concentrations of Pb-based PSCs and $PbCl_2$ for 96 h. The bars represent the median ± SD of three independent experiments, assayed in triplicate. The same lowercase letters above at bar indicate that the results obtained under different exposure concentrations of the same Pb-based PSCs are not significantly different according to the Tukey's test at $P < 0.05$.

well–documented, metal–based NP toxicity may be further mediated by the form of particle (Georgantzopoulou et al., 2016; Nguyen et al., 2018).

4.2. Differences in toxicity sensitivity for Pb-based perovskite solar cells across tested organisms

The toxicity of Pb-based PSCs was assessed in invertebrates, mammalian cells, and bacteria across a wide range of concentrations. All these bioassays shared the objective to find the sensitive species for gaining insights into the potential environmental toxicity of Pb-based PSCs, a promising novel material in the field of PV (Billen et al., 2019; Hauck et al., 2017; Maniarasu et al., 2018; Zhou et al., 2019), both for the ecosystem as well as for humans.

Vibrio fischeri reacted the most sensitively to Pb-based PSCs, followed by soil bacterial communities and *C. elegans* (Fig. 8 and Table 1). This finding coincides with previously reported toxicity studies (Abbas et al., 2018; Parvez et al., 2006; Pino-Otín et al., 2019). An extensive review of the relevant literature indicated that different environmental models varied in their susceptibility to NPs. As example, Khan et al. (2012) proposed the following order of toxicity sensitivity in the pyrene–contaminated soil: *V. fischeri* luminescence inhibition (5 min) > *V. fischeri* luminescence inhibition (15 min) > *Eisenia fetida* mortality (14 and 28 days) > root elongation of *Brassica rapa* (48 h). However, the order of sensitivity for $CH_3NH_3PbI_3$ followed: *D. magna* > *Danio rerio* > *C. elegans* > *Chironomus riparius* (Bae et al., 2019). Recently, increasing efforts have been devoted to screening the most appropriate species with regard to their toxicity sensitivity to NPs and/or contaminants (Bondarenko et al., 2016; Fajardo et al., 2019; Hjorth et al., 2017). The key finding was that *V. fischeri* was generally the most sensitive marker for NP and/or contaminant toxicity, which matched the finding of the present study. However, the turbidity of NP suspensions may limit the light transmission through the suspensions (Hjorth et al., 2017), which would influence the quantification of bioluminescence of *V. fischeri*. A means to account for this is to spike the suspension with *V. fischeri*, which emit a known level of bioluminescence. In this way, the added bacteria can act as an internal standard and the effect of quenching can be estimated and corrected.

In the present study, bacterial communities extracted from soil were sensitive to Pb-based PSCs with EC_{50} values ranging from 8.07 to 12.81 mg L^{-1} (Table 1) according to the Biolog EcoPlate assay. This technique was also suggested as a sensitive tool with which to assess the detrimental effects of NPs (nano–ZnO, –Ag, –Cu, and –Pb) and heavy metals on the metabolic activity of soil microorganisms (Liu et al., 2017; Zhai et al., 2016; Zhai et al., 2017). In general, organisms with higher biomass are less sensitive to toxicants. However, the largest species (*C. elegans*) exhibited the lowest sensitivity to Pb-based PSCs among the tested organisms in this work (Table 1). *Caenorhabditis elegans* is a free–living nematode and a key organism that associates with decomposers and predators in the soil ecosystem (Moon et al., 2019). The observed toxic effects of Pb-based PSC exposure to *C. elegans* were translated into a prominent decrease of viability at 20 mg L^{-1} (Fig. 6). In contrast, exposing human epithelial cell lines to Pb-based PSCs did not significantly reduce their viability. It has been reported before that lanthanum strontium manganite NPs with perovskite structure were non–toxic for airway epithelial cells (Tsai et al., 2019). In contrast to Ag, ZnO, and TiO_2 NPs–induced toxic effects for *P. putida* (Mallevre et al., 2014), the results of the present study indicated that no concentration–dependent toxicity of growth rate and cell viability was observed for *P. putida* (Figs. 3 and S4), which agreed with the previous finding (Esquivel-Gaon et al., 2018).

Interestingly, $CH_3NH_3PbBr_3$ was consistently identified as the most toxic Pb-based PSC in all *in vitro* environmental models in the current study (Table 1). This is consistent with previous *in vitro* studies, all of which demonstrated comparatively higher toxicity of perovskite–based crystal structures (Babayigit et al., 2016; Benmessaoud et al., 2016; Tsai et al., 2019; Zhai et al., 2017; Zhou et al., 2018). A recent study showed that $CH_3NH_3PbI_3$ and its degradation products (PbI_2 and PbO) induced pronounced toxicity, and $CH_3NH_3PbI_3$ was more toxic than its individual degradation products (Bae et al., 2019). The present *in vitro* study showed that the toxicities of $CH_3NH_3PbI_3$ and $NHCHNH_3PbBr_3$ were comparable. The particle size distribution (Fig. 1) and the release of Pb^{2+} from Pb-based PSCs through dissolution (Fig. S3) are hypothesized to play a vital part in the toxic impacts of PSCs. Zhai et al. (2017), Wang et al. (2018), and Moon et al. (2019) stated

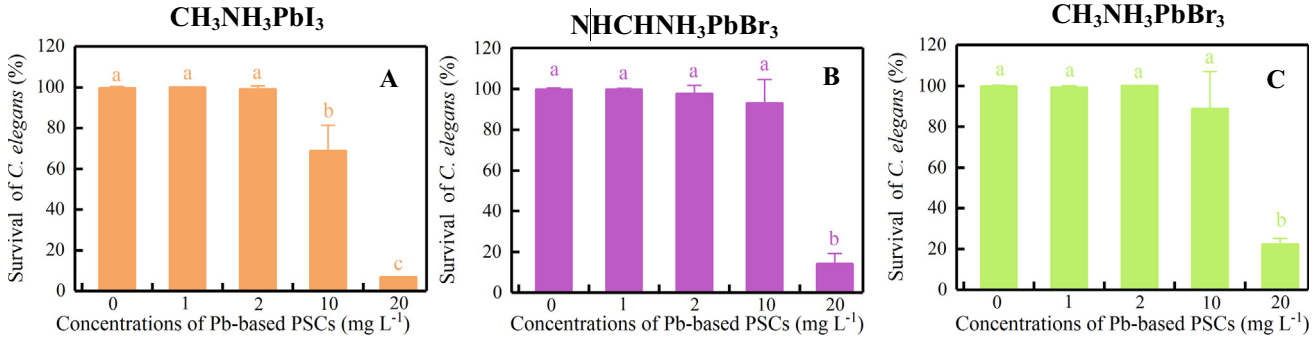

Fig. 6. Effects of Pb-based PSCs on the toxicity to the soil nematode *C. elegans*. The same lowercase in the figure indicates that the results under different exposure concentrations of Pb-based PSCs are not significantly different according to the Tukey's test at $P < 0.05$. Error bars represent standard deviations.

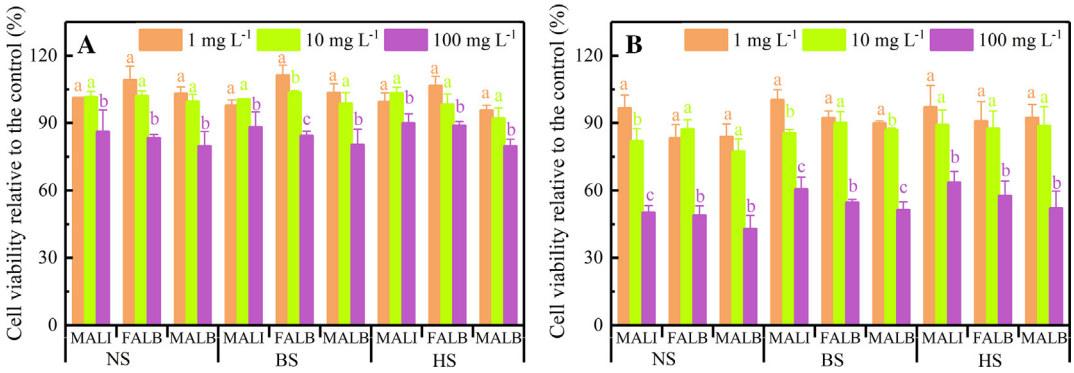

Fig. 7. Cytotoxic effects of Pb-based PSCs on A549 human alveolar epithelial cells (A) and Caco–2/TC7 human colonic epithelial cells (B). MALI, FALB, and MALB are the $CH_3NH_3PbI_3$, $NHCHNH_3PbBr_3$, and $CH_3NH_3PbBr_3$ PSCs, respectively. The data represent the percentage cytotoxicity compared with control cells (exposed to cell culture medium). NS, BS, and HS represent the Pb-based PSCs pre-incubated with no serum added, Bovine serum added, and Human serum added for 1 h at 37 °C, respectively. Graphs represent the mean ± SD derived from at least three independent experiments, assayed in triplicate. The same lowercase above the bar within the same pre–incubated group indicates that the results under different exposure concentrations of the same Pb-based PSCs are not significantly different according to the Tukey's test at $P < 0.05$.

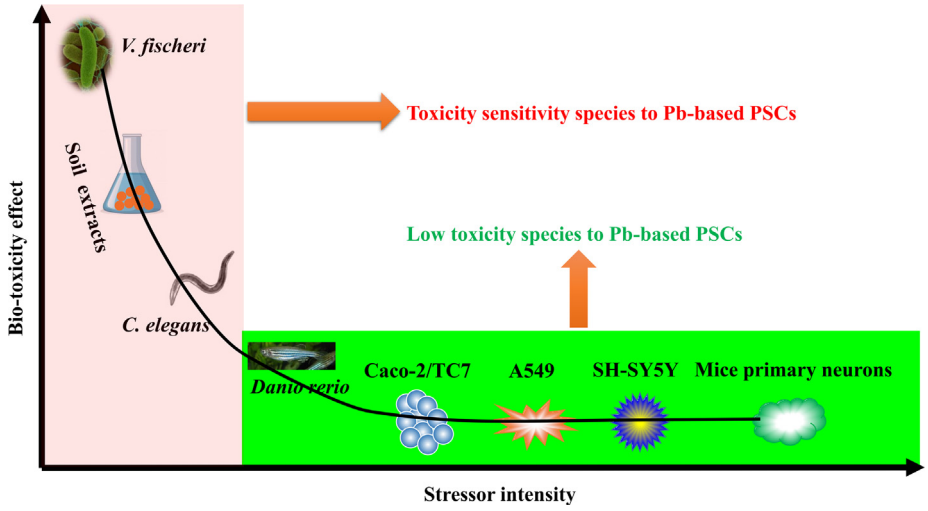

Fig. 8. Schematic diagram of Pb-based PSCs toxicity sensitivity to tested organisms based on the EC_{50} values. The toxicity data of *Danio rerio*, SH–SY5Y, and mice primary neurons were derived from previous literature reports (Babayigit et al., 2016; Benmessaoud et al., 2016).

that, in addition to the released ions, the size of NPs also affects the observed toxicity. A previous study by Dankers et al. (2018) showed that soluble metal oxides release deleterious cations, which mediates toxicity. This indicates why $CH_3NH_3PbBr_3$ was the most sensitive Pb-based PSC to both Caco–2/TC7 cells and soil bacterial communities in the present study, since it is likely that $CH_3NH_3PbBr_3$ showed higher solubility in different exposure media (Fig. S3). Pb remains a public health concern globally, and even low–level Pb exposure potentially leads to various cardiovascular and developmental diseases (Hailegnaw et al., 2015; Kushwaha et al., 2018). Pb^{2+} can enter cells through calcium channels, where it can interact with DNA, thus altering replication, gene transcription, and cell signaling (García-Lestón et al., 2010). Moreover, Pb interferes with the balance of the antioxidant enzymatic system by mediating reactive oxygen species (Ng et al., 2019). However, not only Pb^{2+} is released in the environment upon Pb-based PSC exposure in the environment but also iodide and methylamine (Frost et al., 2014). Interestingly, methylamine has been identified as highly soluble in a water–rich environment and is also known to inhibit fetal development and embryo survival in mice (Guest and Varma, 1991). Therefore, this study suggests that in the search for composites in which Pb^{2+} is substituted by environmentally friendly cations (Sn^{2+}, Cu^{2+}, Ge^{2+}) (Klug et al., 2017; Maniarasu et al., 2018; Zhou et al., 2019), alternatives for the anion should also be considered to replace methylamine.

A multitude of mammalian and environmental models ranging from bacterial (Abbas et al., 2018; Esquivel-Gaon et al., 2018; Mallevre et al., 2014), algal (Bondarenko et al., 2016; Brown et al., 2018; Nguyen et al., 2018), mammalian cells (Brown et al., 2018; Dankers et al., 2018; Muckova et al., 2018), invertebrates, e.g. shellfish, daphnia, nematode (Bacchetta et al., 2018; Barrick et al., 2019; Moon et al., 2019; Ševců et al., 2017; Zhou et al., 2018) and vertebrates, e.g. fish (Babayigit et al., 2016; Ng et al., 2019) can be employed to examine the toxicity of NPs. However, it is impracticable to employ all available models to determine the safety of NPs due to intrinsic shortcomings such as their cost–intensity and time–consumption. Additionally, considering the 3Rs principle (Brown et al., 2018), an increased implementation of alternative models is highly desirable to replace animal testing, as this will be more ethically responsible, cheaper, and easier to perform when assessing the toxicity profile of nanomaterials (Campana and Wlodkowic, 2018; Hristozov et al., 2016). The toxicity data of this work demonstrated *V. fischeri* as the most sensitive organism to Pb-based PSC exposure, followed by soil bacterial communities and *C. elegans* (Fig. 8 and Table 1). Accordingly, priority use of these organisms is recommend since they may

reduce or even replace the requirement for animal testing. Moreover, the underlying assays are rapid and cost–effective means for the efficient screening of the toxicity of Pb-based PSCs as well as NPs in the future.

4.3. Lsimitations of this study

During device fabrication, deployment, and disposal (Hailegnaw et al., 2015), Pb-based PSCs will deposit in soils and waterways, where they will induce the release of toxic Pb^{2+} into the surrounding environment (Babayigit et al., 2016; Zhai et al., 2017). PSCs could therefore exert toxic effects on the entire terrestrial environment. However, the amount of toxicity data of Pb-based PSCs to terrestrial species still remains limited both in previous reports and in the present study. More work is therefore urgently required to further explore the impacts of Pb-based PSCs on terrestrial species such as plants. In addition, only two cell types (representing the lung and colon) were tested due to budgetary constraints of the present work. The toxic responses of other target sites such as the gastrointestinal tract, liver, and kidney were not considered. It is likely that dermal exposure or ingestion of Pb-based PSCs occurs during their production, use, and disposal (Babayigit et al., 2016; Benmessaoud et al., 2016). Previously published literature, clearly indicates that cells from different tissues show large differences in their sensitivity to NPs (Boyes et al., 2017; Kermanizadeh et al., 2016; Pietroiusti et al., 2018). Therefore, a wider array of cell types, representing different target sites, is required to identify differences in cell sensitivity to Pb-based PSC toxicit. This will be beneficial for the development of a comprehensive toxicity assessment strategy and for building a safe by design framework for Pb-based PSCs.

When assessing Pb-based PSC safety, it is important to address the specifics of the toxicity mechanism of photovoltaic perovskites, as these materials clearly pose a potential threat to public health. One of the predominant hallmarks of toxicity could be accompanied by the mediated oxidative stress to cells, which could in turn result in genotoxicity and cytotoxicity (Jalvo et al., 2017; Kermanizadeh et al., 2016; Tsai et al., 2019; Wang et al., 2018). A detailed understanding of the oxidant driven responses of Pb-based PSCs *in vitro* is very important. Moreover, new techniques such as transcriptomics, proteomics, and bioinformatics are currently emerging, which enable the analysis of responses at the molecular signaling level (Georgantzopoulou et al., 2016; Gomes et al., 2019; Khan et al., 2019). These future methods may be able to provide new approaches to predict the mechanisms underlying the toxicity of perovskite exposure.

5. Conclusions

The development of ecologically relevant risk assessment approaches for Pb-based PSCs is impeded because of the scarcity of toxicity data with regard to the effects of Pb-based PSCs on environmental models. To the best of our knowledge, this is the first comparative analysis of the toxicity of Pb-based PSCs for various species, ranging from single aquatic and soil bacterial species and up to more complex forms of life with the aim to assess their environmentally related risk assessment. Overall, *V. fischeri* was the most sensitive organism, followed by soil bacterial communities and *C. elegans*. Considering the technical complexity, standardization status, and sensitivity of the test, the *V. fischeri* test for the assessment of Pb-based PSC toxicity provides the following key merits: operational simplicity, cost–effectiveness, time–saving, excellent reproducibility, as well as reduction/replacement of the use of animal models without ethical concerns. The obtained results stress the potential hazard of large–scale production and application of Pb-based PSCs. The data presented here provides a valuable reference for the safe design of next–generation PSCs by considering alternative, less toxic, ions other than Pb^{2+} and methylamine. Further research on the mechanisms underlying the toxicity of Pb-based PSCs to relevant ecotoxicological models is warranted to obtain a comprehensive picture of the adverse effects of perovskites.

Declaration of Competing Interest

The authors declare that they have no known competing financial interests or personal relationships that could have appeared to influence the work reported in this paper.

Acknowledgments

Guiyin Wang was supported by a grant from the Chinese Scholarship Council (201706910010). This project was supported by the European Union Seventh Framework Programme under EC–GA No. 604602 'FUTURENANONEEDS'. A. S. and P. R. acknowledge the support provided by the Research Infrastructures NanoEnviCz (LM2015073) and Pro-NanoEnviCz (CZ.02.1.01/0.0/0.0/16_013/0001821), supported by the Ministry of Education, Youth and Sports of the Czech Republic. The authors acknowledge Pavel Kejzlar (TUL) for the SEM analyses. The authors extremely thank the anonymous reviewers for their helpful comments and MogoEdit, China (http://en.mogoedit.com/), for improving the language of this manuscript.

Appendix A. Supplementary data

Supplementary data to this article can be found online at https://doi.org/10.1016/j.scitotenv.2019.135134.

References

Abbas, M., Adil, M., Ehtisham-ul-Haque, S., Munir, B., Yameen, M., Ghaffar, A., Shar, G.A., Asif, Tahir M., Iqbal, M., 2018. *Vibrio fischeri* bioluminescence inhibition assay for ecotoxicity assessment: a review. Sci. Total Environ. 626, 1295–1309.

Alaaeddin, M.H., Sapuan, S.M., Zuhri, M.Y.M., Zainudin, E.S., AL-Oqla, F.M., 2019. Photovoltaic applications: status and manufacturing prospects. Renew. Sust. Energ. Rev. 102, 318–332.

Babayigit, A., Duy, Thanh D., Ethirajan, A., Manca, J., Muller, M., Boyen, H., Conings, B., 2016. Assessing the toxicity of Pb- and Sn-based perovskite solar cells in model organism *Danio rerio*. Sci. Rep. 6, 18721.

Bacchetta, R., Santo, N., Valenti, I., Maggioni, D., Longhi, M., Tremolada, P., 2018. Comparative toxicity of three differently shaped carbon nanomaterials on *Daphnia magna*: Does a shape effect exist?. Nanotoxicology 12, 201–223.

Baderna, D., Colombo, A., Romeo, M., Cambria, F., Teoldi, F., Lodi, M., Diomede, L., Benfenati, E., 2014. Soil quality in the Lomellina area using *in vitro* models and ecotoxicological assays. Environ. Res. 133, 220–231.

Bae, S., Lee, S.Y., Kim, J., Umh, H.N., Jeong, J., Bae, S., Yi, J., Kim, Y., Choi, J., 2019. Hazard potential of perovskite solar cell technology for potential implementation of "safe-by-design" approach. Sci. Rep. 9, 4242.

Barrick, A., Manier, N., Lonchambon, P., Flahaut, E., Jrad, N., Mouneyrac, C., Châtel, A., 2019. Investigating a transcriptomic approach on marine mussel hemocytes exposed to carbon nanofibers: An in vitro/in vivo comparison. Aquat. Toxicol. 207, 19–28.

Benmessaoud, I.R., Mahul-Mellier, A., Horváth, E., Bohumil, M., Massimo, S., Lashuel, H.A., Forró, L., 2016. Health hazards of methylammonium lead iodide based perovskites: cytotoxicity studies. Toxicol. Res. 5, 407.

Billen, P., Leccisi, E., Dastidar, S., Li, S., Lobaton, L., Spatari, S., Fafarman, A.T., Fthenakis, V.M., Baxter, J.B., 2019. Comparative evaluation of lead emissions and toxicity potential in the life cycle of lead halide perovskite photovoltaics. Energy 166, 1089–1096.

Bondarenko, O.M., Heinlaan, M., Sihtmäe, M., Ivask, A., Kurvet, I., Joonas, E., Jemec, A., Mannerström, M., Heinonen, T., Rekulapelly, R., Singh, S., Zou, J., Pyykkö, I., Drobne, D., Kahru, A., 2016. Multilaboratory evaluation of 15 bioassays for (eco)toxicity screening and hazard ranking of engineered nanomaterials: FP7 project NANOVALID. Nanotoxicology 10, 1229–1242.

Boyes, W.K., Thornton, B., Al-Abed, S.R., Andersen, C.P., Bouchard, D.C., Burgess, R.M., Hubal, E., Ho, K.T., Hughes, M.F., Kitchin, K., Reichman, J.R., Rogers, K.R., Ross, J. A., Rygiewicz, P.T., Scheckel, K.G., Thai, S.F., Zepp, R.G., Zucker, R.M., 2017. A comprehensive framework for evaluating the environmental health and safety implications of engineered nanomaterials. Crit. Rew. Toxicol. 47, 767–810.

Brown, D.M., Johnston, H.J., Gaiser, B., Pinna, N., Caputo, G., Culha, M., Kelestemur, S., Altunbek, M., Stone, V., Roy, J.C., Kinross, J.H., Fernandes, T.F., 2018. A cross-species and model comparison of the acute toxicity of nanoparticles used in the pigment and ink industries. NanoImpact 11, 20–32.

Campana, O., Wlodkowic, D., 2018. The undiscovered country: ecotoxicology meets microfluidics. Sensor. Actuat. B Chem. 257, 692–704.

Celik, I., Song, Z., Phillips, A.B., Heben, M.J., Apul, D., 2018. Life cycle analysis of metals in emerging photovoltaic (PV) technologies: a modeling approach to estimate use phase leaching. J. Clean. Prod. 186, 632–639.

Chen, M., Ju, M., Garces, H.F., Carl, A.D., Ono, L.K., Hawash, Z., Zhang, Y., Shen, T., Qi, Y., Grimm, R.L., Pacifici, D., Zeng, X.C., Zhou, Y., Padture, N.P., 2019. Highly stable and efficient all-inorganic lead-free perovskite solar cells with native-oxide passivation. Nat. Commun. 10, 16.

Dankers, A.C.A., Kuper, C.F., Boumeester, A.J., Fabriek, B.O., Kooter, I.M., Gröllers-Mulderij, M., Tromp, P., Nelissen, I., Zondervan-Van Den Beuken, E.K., Vandebriel, R.J., 2018. A practical approach to assess inhalation toxicity of metal oxide nanoparticles in vitro. J. Appl. Toxicol. 38, 160–171.

Deary, M.E., Ekumankama, C.C., Cummings, S.P., 2018. Effect of lead, cadmium, and mercury co-contaminants on biodegradation in PAH-polluted soils. Land Degrad. Dev. 29, 1583–1594.

Esquivel-Gaon, M., Nguyen, N.H.A., Sgroi, M.F., Pullini, D., Gili, F., Mangherini, D., Pruna, A.I., Rosicka, P., Sevcu, A., Castagnola, V., 2018. In vitro and environmental toxicity of reduced graphene oxide as an additive in automotive lubricants. Nanoscale 10, 6539–6548.

Fajardo, C., Costa, G., Nande, M., Martín, C., Martín, M., Sánchez-Fortún, S., 2019. Heavy metals immobilization capability of two iron-based nanoparticles (nZVI and Fe_3O_4): soil and freshwater bioassays to assess ecotoxicological impact. Sci. Total Environ. 656, 421–432.

Frost, J.M., Butler, K.T., Brivio, F., Hendon, C.H., van Schilfgaarde, M., Walsh, A., 2014. Atomistic origins of high-performance in hybrid halide perovskite solar cells. Nano Lett. 14, 2584–2590.

García-Lestón, J., Méndez, J., Pásaro, E., Laffon, B., 2010. Genotoxic effects of lead: an updated review. Environ. Int. 36, 623–636.

Georgantzopoulou, A., Serchi, T., Cambier, S., Leclercq, C.C., Renaut, J., Shao, J., Kruszewski, M., Lentzen, E., Grysan, P., Eswara, S., Audinot, J.-N., Contal, S., Ziebel, J., Guignard, C., Hoffmann, L., Murk, A.J., Gutleb, A.C., 2016a. Effects of silver nanoparticles and ions on a co-culture model for the gastrointestinal epithelium. Part. Fibre Toxicol. 13, 9.

Georgantzopoulou, A., Cambier, S., Serchi, T., Kruszewski, M., Balachandran, Y.L., Lentzen, E., Grysan, P., Audinot, J.-N., Ziebel, J., Guignard, C., Gutleb, A.C., Murk, A.J., 2016b. Inhibition of multixenobiotic resistance (MXR) transporters by silver nanoparticles and -ions in vitro and in *Daphnia magna*. Sci. Total Environ. 569–570, 681–689.

Gomes, S.I.L., Roca, C.P., Scott-Fordsmand, J.J., Amorim, M.J.B., 2019. High-throughput transcriptomics: insights into the pathways involved in (nano) nickel toxicity in a key invertebrate test species. Environ. Pollut. 245, 131–140.

Guest, I., Varma, D.R., 1991. Developmental toxicity of methylamines in mice. J. Toxicol. Environ. Health 32, 319–330.

Hailegnaw, B., Kirmayer, S., Edri, E., Hodes, G., Cahen, D., 2015. Rain on methylammonium lead iodide based perovskites: Possible environmental effects of perovskite solar cells. J. Phys. Chem. Lett. 6, 1543–1547.

Hauck, M., Ligthart, T., Schaap, M., Boukris, E., Brouwer, D., 2017. Environmental benefits of reduced electricity use exceed impacts from lead use for perovskite based tandem solar cell. Renew. Energ. 111, 906–913.

Hristozov, D., Gottardo, S., Semenzin, E., Oomen, A., Bos, P., Peijnenburg, W., van Tongeren, M., Nowack, B., Hunt, N., Brunelli, A., Scott-Fordsmand, J.J., Tran, L., Marcomini, A., 2016. Frameworks and tools for risk assessment of manufactured nanomaterials. Environ. Int. 95, 36–53.

Hjorth, R., Coutris, C., Nguyen, N.H.A., Sevcu, A., Gallego-Urrea, J.A., Baun, A., Joner, E. J., 2017. Ecotoxicity testing and environmental risk assessment of iron nanomaterials for sub-surface remediation – Recommendations from the FP7 project NanoRem. Chemosphere 182, 525–531.

Iannarelli, L., Giovannozzi, M.A., Morelli, F., Viscotti, F., Bigini, P., Maurino, V., Spoto, G., Martra, G., Ortel, E., Hodoroaba, V.D., Rossi, A.M., Diomede, L., 2016. Shape engineered TiO_2 nanoparticles in *Caenorhabditis elegans*: a Raman imaging based approach to assist tissue-specific toxicological studies. RSC Adv. 6, 70501–70509.

ISO, 1999. Water quality—evaluation of ultimate aerobic biodegradability of organic compounds in aqueous medium by determination of oxygen demand in a closed respirometer. ISO 9408. International Standardization Organization, Geneva, Switzerland.

ISO, 2007. Water quality—determination of the inhibitory effect of water samples on the light emission of vibrio fischeri (luminescent bacteria test) part 3: method using freeze-dried bacteria. ISO 11348-3. International Organisation for Standardization Geneva, Switzerland.

ISO, 2010. Water quality—determination of the toxic effect of sediment and soil samples on growth, fertility and reproduction of Caenorhabditis elegans (Nematoda). ISO 10872. International Organization for Standardization Geneva, Switzerland.

Jalvo, B., Faraldos, M., Bahamonde, A., Rosal, R., 2017. Antimicrobial and antibiofilm efficacy of self-cleaning surfaces functionalized by TiO_2 photocatalytic nanoparticles against *Staphylococcus aureus* and *Pseudomonas putida*. J. Hazard. Mater. 340, 160–170.

Jeon, N.J., Na, H., Jung, E.H., Yang, T., Lee, Y.G., Kim, G., Shin, H., Il, Seok S., Lee, J., Seo, J., 2018. A fluorene-terminated hole-transporting material for highly efficient and stable perovskite solar cells. Nat. Energy 3, 682–689.

Jensen, K.A., Kembouche, Y., Christiansen, E., Jacobsen, N.R., Wallin, H., Guiot, C., Spalla, O., Witschger, O., 2011. Final protocol for producing suitable manufactured nanomaterial exposuremedia. Web-Report. The generic NANOGENOTOX dispersion protocol - Standard Operation Procedure (SOP). October, 2011.

Kayesh, M.E., Chowdhury, T.H., Matsuishi, K., Kaneko, R., Kazaoui, S., Lee, J., Noda, T., Islam, A., 2018. Enhanced photovoltaic performance of $FASnI_3$-based perovskite solar cells with hydrazinium chloride coadditive. ACS Energy Lett. 3, 1584–1589.

Klein, S., Cambier, S., Hennen, J., Legay, S., Serchi, T., Nelissen, I., Chary, A., Moschini, E., Krein, A., Blömeke, B., Gutleb, A.C., 2017. Endothelial responses of the alveolar barrier in vitro in a dose-controlled exposure to diesel exhaust particulate matter. Part. Fibre Toxicol. 14, 7.

Kermanizadeh, A., Gosens, I., MacCalman, L., Johnston, H., Danielsen, P.H., Jacobsen, N.R., Lenz, A., Fernandes, T., Schins, R.P.F., Cassee, F.R., Info, E.D.N., Wallin, H., Kreyling, W., Stoeger, T., Loft, S., Møller, P., Tran, L., Stone, V., 2016. A multilaboratory toxicological assessment of a panel of 10 engineered nanomaterials to human health-ENPRA project-the highlights, limitations, and current and future challenges. J. Toxicol. Env. Heal. B 19, 1–28.

Khan, A.M., Korzeniowska, B., Gorshkov, V., Tahir, M., Schrøder, H., Skytte, L., Rasmussen, K.L., Khandige, S., Møller-Jensen, J., Kjeldsen, F., 2019. Silver nanoparticle-induced expression of proteins related to oxidative stress and neurodegeneration in an in vitro human blood-brain barrier model. Nanotoxicology. https://doi.org/10.1080/17435390.2018.1540728.

Khan, M.I., Cheema, S.A., Tang, X., Shen, C., Sahi, S.T., Jabbar, A., Park, J., Chen, Y., 2012. Biotoxicity assessment of pyrene in soil using a battery of biological assays. Arch. Environ. Con. Tox. 63, 503–512.

Klug, M.T., Osherov, A., Haghighirad, A.A., Stranks, S.D., Brown, P.R., Bai, S., Wang, J.T. W., Dang, X., Bulović, V., Snaith, H.J., Belcher, A.M., 2017. Tailoring metal halide perovskites through metal substitution: influence on photovoltaic and material properties. Energy Environ. Sci. 10, 236–246.

Kushwaha, A., Hans, N., Kumar, S., Rani, R., 2018. A critical review on speciation, mobilization and toxicity of lead in soil-microbe-plant system and bioremediation strategies. Ecotox. Environ. Safe. 147, 1035–1045.

Liu, B., Li, Y., Gao, S., Chen, X., 2017. Copper exposure to soil under single and repeated application: Selection for the microbial community tolerance and effects on the dissipation of antibiotics. J. Hazard. Mater. 325, 129–135.

Mallevre, F., Fernandes, T.F., Aspray, T.J., 2014. Silver, zinc oxide and titanium dioxide nanoparticle ecotoxicity to bioluminescent *Pseudomonas putida* in laboratory medium and artificial wastewater. Environ. Pollut. 195, 218–225.

Maniarasu, S., Korukonda, T.B., Manjunath, V., Ramasamy, E., Ramesh, M., Veerappan, G., 2018. Recent advancement in metal cathode and hole-conductor-free perovskite solar cells for low-cost and high stability: a route towards commercialization. Renew. Sust. Energ. Rev. 82, 845–857.

Moon, J., Kwak, J.I., An, Y., 2019. The effects of silver nanomaterial shape and size on toxicity to *Caenorhabditis elegans* in soil media. Chemosphere 215, 50–56.

Muckova, L., Pejchal, J., Jost, P., Vanova, N., Herman, D., Jun, D., 2018. Cytotoxicity of acetylcholinesterase reactivators evaluated in vitro and its relation to their structure. Drug Chem. Toxicol. 42, 1–5.

Nguyen, N.H.A., Špánek, R., Kasalický, V., Ribas, D., Vlková, D., Řeháková, H., Kejzlar, P., Ševců, A., 2018a. Different effects of nano-scale and micro-scale zero-valent iron particles on planktonic microorganisms from natural reservoir water. Environ. Sci. Nano 5, 1117–1129.

Nguyen, N.H.A., Padil, V.V.T., Slaveykova, V.I., Černík, M., Ševců, A., 2018b. Green synthesis of metal and metal oxide nanoparticles and their effect on the unicellular alga *Chlamydomonas reinhardtii*. Nanoscale Res. Lett. 13, 159.

Ng, D., Chu, Y., Tan, S., Wang, S., Lin, Y., Chu, C., Soo, Y., Song, Y., Chen, P., 2019. In vivo evidence of intestinal lead dissolution from lead dioxide (PbO_2) nanoparticles and resulting bioaccumulation and toxicity in medaka fish. Environ. Sci. Nano 6, 580.

OECD, 2013. Guidelines for the Testing of Chemicals, Test No. 236: Fish Embryo Acute Toxicity (FET) Test. OECD Publishing, Paris.

Oztig, L.I., 2017. Europe's climate change policies: the Paris agreement and beyond. Energ. Source. Part B 12, 917–924.

Parvez, S., Venkataraman, C., Mukherji, S., 2006. A review on advantages of implementing luminescence inhibition test (*Vibrio fischeri*) for acute toxicity prediction of chemicals. Environ. Int. 32, 265–268.

Pietroiusti, A., Stockmann-Juvala, H., Lucaroni, F., Savolainen, K., 2018. Nanomaterial exposure, toxicity, and impact on human health. WIREs Nanomed. Nanobiotechnol. 10, 1513.

Pino-Otín, M.R., Ballestero, D., Navarro, E., González-Coloma, A., Val, J., Mainar, A.M., 2019. Ecotoxicity of a novel biopesticide from *Artemisia absinthium* on non-target aquatic organisms. Chemosphere 216, 131–146.

Shah, A.A., Khan, A., Dwivedi, S., Musarrat, J., Azam, A., 2018. Antibacterial and antibiofilm activity of barium titanate nanoparticles. Mater. Lett. 229, 130–133.

Ševců, A., El-Temsah, Y.S., Filip, J., Joner, E.J., Bobčíková, K., Černík, M., 2017. Zero-valent iron particles for PCB degradation and an evaluation of their effects on bacteria, plants, and soil organisms. Environ. Sci. Pollut. R. 24, 21191–21202.

Tavakoli, M.M., Zakeeruddin, S.M., Grätzel, M., Fan, Z., 2018. Large-grain tin-rich perovskite films for efficient solar cells via metal alloying technique. Adv. Mater. 30, 1705998.

Tsai, S., Mesina, M., Goshia, T., Chiu, M., Young, J., Sibal, A., Chin, W., 2019. Perovskite nanoparticles toxicity study on airway epithelial cells. Nanoscale Res. Lett. 14, 14.

Wang, B., Zhang, J., Chen, C., Xu, G., Qin, X., Hong, Y., Bose, D.D., Qiu, F., Zou, Z., 2018. The size of zinc oxide nanoparticles controls its toxicity through impairing autophagic flux in A549 lung epithelial cells. Toxicol. Lett. 285, 51–59.

Zhai, Y., Hunting, E.R., Wouters, M., Peijnenburg, W.J.G.M., Vijver, M.G., 2016. Silver nanoparticles, ions, and shape governing soil microbial functional diversity: Nano shapes micro. Front. Microbiol. 7, 1123.

Zhai, Y., Hunting, E.R., Wouterse, M., Peijnenburg, W.J.G.M., Vijver, M.G., 2017. Importance of exposure dynamics of metal-based nano-ZnO, -Cu and -Pb governing the metabolic potential of soil bacterial communities. Ecotox. Environ. Safe. 145, 349–358.

Zhou, T., Fan, W., Liu, Y., Wang, X., 2018. Comparative assessment of the chronic effects of five nano-perovskites on *Daphnia magna*: A structure-based toxicity mechanism. Environ. Sci. Nano 5, 708–719.

Zhou, T., Wang, M., Zang, Z., Tang, X., Fang, L., 2019. Two-dimensional lead-free hybrid halide perovskite using superatom anions with tunable electronic properties. Sol. Energ. Mat. Sol. C. 191, 33–38.